

Waveguide-Based 1.5 μm Optical Isolator Based on Magneto-Optic Effect in Ferromagnetic MnAs

This content has been downloaded from IOPscience. Please scroll down to see the full text.

2007 Jpn. J. Appl. Phys. 46 205

(<http://iopscience.iop.org/1347-4065/46/1R/205>)

View [the table of contents for this issue](#), or go to the [journal homepage](#) for more

Download details:

IP Address: 131.112.10.178

This content was downloaded on 19/07/2017 at 16:37

Please note that [terms and conditions apply](#).

You may also be interested in:

[Semiconductor Waveguide Optical Isolator Incorporating Ferromagnetic Epitaxial MnSb for High Temperature Operation](#)

Tomohiro Amemiya, Yusuke Ogawa, Hiromasa Shimizu et al.

[Substrate-Orientation Dependence on Structure and Magnetic Properties of MnAs Epitaxial Layers](#)

Yoshitaka Morishita, Koichi Iida, Junya Abe et al.

[Longitudinal Magneto-Optic Effect in Ferromagnetic Thin Films. I](#)

Toshihiko Yoshino and Shun-ichi Tanaka

[Optical Waveguide in GaAs by Drive-in Diffusion Technique](#)

Shigeaki Ohke, Yasuhisa Ida, Akira Kusunoki et al.

[Longitudinal Magneto-Optic Effect in Ferromagnetic Thin Films. II](#)

Shun-ichi Tanaka, Toshihiko Yoshino and Tsunehiko Takahashi

[Waveguiding Characteristics of Optical Waveguide with Claddings Having Negative Nonlinear Refractive Coefficient](#)

Shigeaki Ohke, Yutaka Satomura, Tokuo Umeda et al.

[Gradient Index Polymer Optical Waveguide Patterned by Ultraviolet Irradiation](#)

Shuji Eguchi, Hideki Asano, Atsusi Kannke et al.

[Growth Direction Control of Ferromagnetic MnAs Grown by Selective-Area Metal–Organic Vapor Phase Epitaxy](#)

Toshitomo Wakatsuki, Shinjiro Hara, Shingo Ito et al.

Waveguide-Based 1.5 μm Optical Isolator Based on Magneto-Optic Effect in Ferromagnetic MnAs

Tomohiro AMEMIYA^{1,3*}, Hiromasa SHIMIZU^{1,3}, Pham Nam HAI^{2,3},
Masafumi YOKOYAMA^{2,3}, Masaaki TANAKA^{2,3}, and Yoshiaki NAKANO^{1,3}

¹Research Center for Advanced Science and Technology, 4-6-1 Komaba, Meguro-ku, Tokyo 153-8904, Japan

²Department of Electronic Engineering, The University of Tokyo, 7-3-1 Hongo, Bunkyo-ku, Tokyo 113-8656, Japan

³Japan Science and Technology Agency, SORST

(Received August 13, 2006; accepted September 24, 2006; published online January 10, 2007)

We developed a 1.5- μm -band, transverse-magnetic-mode waveguide isolator based on the nonreciprocal-loss phenomenon. The device consists of an optical waveguide with an InGaAs/InGaAlAs multiple-quantum-well amplifier and a ferromagnetic MnAs layer attached to the waveguide. The combination of the optical waveguide and the magnetized MnAs layer produces a magneto-optic effect called the nonreciprocal loss—a phenomenon where the propagation loss of light is larger in backward than in forward propagation. We present the guiding principle of the design of the structure of the device. A prototype device with a MBE-grown epitaxial MnAs layer showed a nonreciprocity of 9.8 dB/mm at a wavelength of 1.54 μm . Our device can be monolithically integrated with waveguide-based optical devices on an InP substrate. [DOI: 10.1143/JJAP.46.205]

KEYWORDS: waveguide optical isolator, magneto-optic effect, nonreciprocal loss, semiconductor optical amplifier, ferromagnetic, MnAs, photonic integrated circuit

1. Introduction

A promising area of research on optical communication systems is the development of photonic integrated circuits that combine a variety of optical devices on a chip. To construct such integrated circuits, we need to develop small-sized waveguide isolators that can be monolithically combined with waveguide-based optical devices. In this paper, we propose one such device, a 1.5- μm -band waveguide isolator that consists of a III–V semiconductor waveguide combined with a ferromagnetic manganese arsenide (MnAs) layer. The device produces optical nonreciprocity that is based on a magneto-optic phenomenon called the *nonreciprocal loss*.

Optical isolators are indispensable elements in photonic integrated circuits for interconnecting different optical devices in a cascade manner without problems caused by undesirable reflections of light in the circuit. Isolators are required to have the form of a waveguide because they must be monolithically combined with waveguide-based optical devices such as semiconductor lasers, light amplifiers, and switches. Conventional optical isolators, however, cannot meet this requirement because they are composed of Faraday rotators and polarizers, which are difficult to integrate with waveguide-based devices. For this reason, much effort has been expended in developing waveguide optical isolators.^{1–6)} However, most of the reported devices use ferromagnetic iron garnets to produce nonreciprocity in light propagation, and therefore they are incompatible with semiconductor optical devices.

One promising way of creating waveguide-based semiconductor isolators is by the use of the nonreciprocal loss phenomenon where—in an optical waveguide with a magnetized metal layer—the propagation loss of light is larger in backward than in forward propagation.^{7,8)} The use of this phenomenon can provide semiconductor waveguide isolators that are suitable for monolithic integration with other semiconductor optical devices. The leading example

was reported by Vanwolleghem *et al.*^{9,10)} Their device consists of an InGaAlAs/InP active waveguide with a ferromagnetic CoFe layer for producing nonreciprocity and operates at a 1.3 μm transverse-magnetic (TM) mode.

To construct 1.55 μm , polarization-independent waveguide isolators for optical communication systems, we are developing transverse-electric-mode (TE-mode) and TM-mode isolators based on the nonreciprocal loss at a 1.55 μm wavelength. We have built a prototype of a TE-mode isolator, consisting of an InGaAsP/InP active waveguide combined with a ferromagnetic Fe layer for nonreciprocity, and obtained a nonreciprocity of 14.7 dB/mm—the largest value ever reported for waveguide isolators.^{11,12)} Encouraged by this result, we then considered a TM-mode waveguide isolator and, in the previous paper, reported the idea of constructing the device by using ferromagnetic MnAs instead of Fe-based metals.^{13,14)} However, the structure of our previous device was not optimized because, at that time, we had no detailed data on the magneto-optic properties of MnAs at a 1.5 μm wavelength. After that, we measured the dielectric tensor of magnetized MnAs at 1.5 μm . Using this data, we redesigned the device and obtained a nonreciprocity of 9.8 dB/mm at a 1.54 μm wavelength. The following sections provide the details on this TM-mode isolator.

2. Structure of the TM-Mode Waveguide Isolator

Figure 1 shows our TM-mode waveguide isolator with a cross section perpendicular to the direction of light propagation. The device consists of a TM-mode semiconductor optical-amplifying waveguide (SOA waveguide) on an InP substrate and a ferromagnetic MnAs layer attached to the SOA waveguide. The SOA consists of an InGaAs/InGaAlAs multiple quantum well (MQW) sandwiched between two InGaAlAs guiding layers. The upper guiding layer is covered with an InP cladding layer and then an InGaAsP contact layer; a thin cladding layer is used so that light traveling in the SOA waveguide can extend into the MnAs layer to interact with the magnetic moment in the MnAs layer. An Au/Ti double metal layer covers the MnAs layer, forming a top electrode to supply the driving current

*Corresponding author. E-mail address: ametomo@hotaka.t.u-tokyo.ac.jp

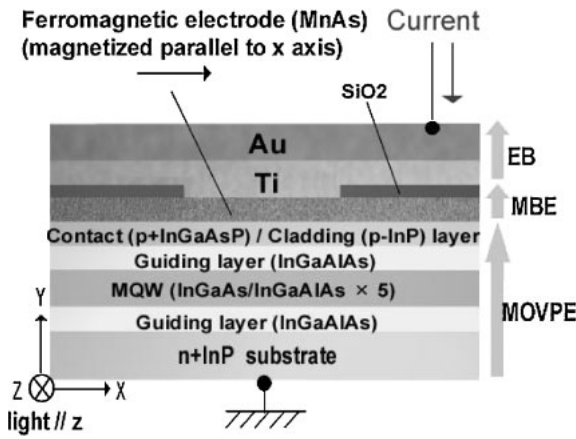


Fig. 1. Structure (cross section) of the TM-mode waveguide optical isolator with a MnAs layer magnetized in the x -direction and light passing along the z -direction.

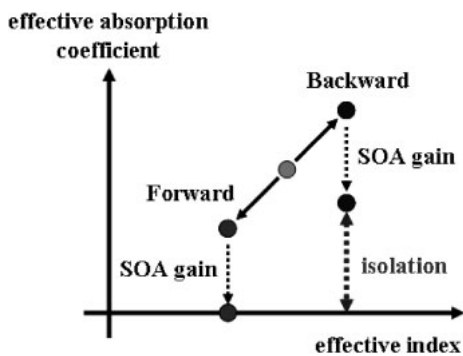


Fig. 2. Principle of the operation of the isolator based on the non-reciprocal loss.

to the SOA. Incident light passes through the SOA waveguide perpendicular to the figure (z -direction).

To operate the device, an external magnetic field is applied so that the MnAs layer is magnetized perpendicular to the propagation of light, as indicated by the arrow in the figure (x -direction). Light traveling in the device interacts with magnetic moments in the MnAs layer. This produces a difference in the propagation loss of TM-polarized light between forward (z -direction) and backward propagation ($-z$ -direction); the propagation loss is larger for backward propagation than for forward propagation, as shown in Fig. 2. This nonreciprocal loss is caused by the magneto-optic transverse Kerr effect. The SOA compensates for the forward propagation loss; it is operated so that the net loss for forward propagation is zero (see Fig. 2). Under these conditions, the device can act as an optical isolator.

The point of our device is its use of MnAs as a ferromagnetic material, instead of ferromagnetic metals such as Fe, Co, and Ni. In our device structure—which is necessary for TM-mode operation—the ferromagnetic layer used to produce the nonreciprocity is also used as a contact to supply a driving current to the SOA. This means that the ferromagnetic layer has to meet a dual requirement of producing a large Kerr effect and of providing a low-resistance contact for the p-type InGaAsP contact layer. Ordinary ferromagnetic metals are not suited for this purpose because they produce a Schottky barrier on p-type

InGaAsP, thereby producing a high-resistance contact on the contact layer (see §5). In addition, during contact annealing, they produce undesirable nonferromagnetic compounds such as FeAs and NiAs at the contact interface and simultaneously degrade the microscopic flatness of the interface; this reduces optical nonreciprocity in the device. To solve these problems, we used MnAs for the ferromagnetic layer, which is a ferromagnetic, intermetallic compound with a hexagonal NiAs structure. It can be grown epitaxially on GaAs, InP, and related semiconductors by using molecular beam epitaxy (MBE), without producing a solid-phase reaction at the interface.^{15–17} It also produces no Schottky barrier on p-type InGaAsP.

We designed a SOA structure for use at a $1.5\mu\text{m}$ wavelength. The resultant structure is as follows. The substrate is a highly doped n-type InP (refractive index $n = 3.16$). The constituent layers of the SOA are: (i) lower guiding layer: 100-nm-thick InGaAlAs (bandgap wavelength $\lambda_g = 1.1\mu\text{m}$, $n = 3.39$), (ii) MQW: five tensile-strained InGaAs quantum wells (-0.4% strained, 15-nm-thick well, $n_{\text{MQW}} = 3.53$) with six compressively strained InGaAlAs barriers ($+0.6\%$ strained, 12-nm-thick barrier, $\lambda_g = 1.2\mu\text{m}$), (iii) upper guiding layer: 100-nm-thick InGaAlAs ($\lambda_g = 1.1\mu\text{m}$), (iv) cladding layer: 200-nm-thick p-type InP, and (v) contact layer: 250-nm-thick, highly doped p-type InGaAsP ($\lambda_g = 1.4\mu\text{m}$). The thickness of the MnAs layer affects the strength of the interaction between light in the SOA and magnetic moments in the MnAs layer. We determined the optimum thickness of the MnAs layer through the following calculation.

3. Measuring the Magneto-Optic Properties of MnAs Layers

Light traveling along the SOA waveguide extends beyond the interface into the MnAs layer to a certain penetration depth and interacts with magnetic moments in the MnAs layer. To produce optical nonreciprocity effectively, the thickness of the MnAs layer must be set larger than the penetration depth. However, using existing epitaxial technology, it is difficult to grow a high-quality MnAs layer with a thickness of several hundred nanometers. Therefore, when designing the device, we must ascertain whether sufficient nonreciprocity can be obtained with the small MnAs thickness we can produce. For this purpose, we calculated the isolation ratio of the device as a function of the MnAs thickness by computer simulation using the dielectric tensor data of MnAs. The simulation results are compared with measurement data in §5.

The nonreciprocity of our isolator is caused by the off-diagonal elements in the dielectric tensor of the ferromagnetic MnAs. The dielectric tensor of each layer in Fig. 1(a) is given by

$$\begin{pmatrix} \varepsilon_n & 0 & 0 \\ 0 & \varepsilon_n & j\alpha_n \\ 0 & -j\alpha_n & \varepsilon_n \end{pmatrix}, \quad (1)$$

where ε_n and α_n are the diagonal and the off-diagonal elements of the dielectric tensor in the n th layer, respectively. The off-diagonal element α_n is 0 except in the MnAs layer. Using the dielectric tensors, Maxwell's equations give the transfer matrix for each layer. We find from the transfer

matrix that magnetic field H_x (parallel to x axis), electric field E_z (parallel to z axis), and propagation coefficient β are given by

$$\begin{pmatrix} H_x|_{\text{top}} \\ \omega\epsilon_0 E_z|_{\text{top}} \end{pmatrix} = \left(\prod_{\text{All}} \mathbf{M}_n \right) \begin{pmatrix} H_x|_{\text{bottom}} \\ \omega\epsilon_0 E_z|_{\text{bottom}} \end{pmatrix} \quad (2)$$

$$\mathbf{M}_n = \begin{pmatrix} \cosh(\beta_n d_n) + \frac{\alpha_n \beta}{\beta_n \epsilon_n} \sinh(\beta_n d_n) & \frac{\epsilon_n^2 - \alpha_n^2}{j\beta_n \epsilon_n} \sinh(\beta_n d_n) \\ \frac{j}{\epsilon_n^2 - \alpha_n^2} \left(\beta_n \epsilon_n - \frac{(\alpha_n \beta)^2}{\beta_n \epsilon_n} \right) \sinh(\beta_n d_n) & \cosh(\beta_n d_n) - \frac{\alpha_n \beta}{\beta_n \epsilon_n} \sinh(\beta_n d_n) \end{pmatrix} \quad (\beta_n = \sqrt{\beta^2 - k_0^2 \epsilon_n}),$$

where $H_x|_{\text{top}}$ and $E_z|_{\text{top}}$ are the magnetic field and the electric field at the bottom of the Au electrode, and $H_x|_{\text{bottom}}$ and $E_z|_{\text{bottom}}$ are the magnetic field and the electric field at the top of the InP substrate, respectively, and d_n is the thickness of the n th layer. Because of the nonzero off-diagonal elements of MnAs, the equation for backward-propagating TM waves is different from that of forward TM waves; this leads to a nonreciprocal solution for the propagation coefficient β . The nonreciprocal solution gives the difference in absorption coefficient between forward (z direction) and backward ($-z$ direction) TM waves, and therefore, gives the isolation ratio (or the difference between forward absorption and backward absorption) in our device.

The dielectric tensor of MnAs for a 1.5 μm wavelength was needed in this calculation, but no available data had been reported; only the tensor for the visible wavelength range had been reported.¹⁸⁾ Therefore, we measured the values of the tensor elements. The diagonal element of the tensor can be determined from the complex refractive index, and the off-diagonal element can be determined from the Faraday rotation and the Faraday ellipticity. To measure these values for a MnAs layer, we prepared two samples, i.e., a 20-nm-thick layer and a 50-nm-thick MnAs layer grown by MBE on a 200- μm -thick, [100]-oriented GaAs substrate (the back was mirror-polished in both samples). The complex refractive index was obtained from the reflection data for the samples and the difference in transmission data between the samples. The Faraday rotation and the Faraday ellipticity were obtained from the difference in transmission data between the two samples which were magnetized perpendicular to the layer surface. Figure 3(a) shows a plot of the measured complex refractive index $n + ik$ ($= \epsilon_n|_{\text{MnAs}}^{1/2}$) as a function of wavelength. Figure 3(b) shows a plot of the off-diagonal element ϵ_{yz} ($= j\alpha_n|_{\text{MnAs}}$), where $\text{Re}(\epsilon_{yz})$ is the real part and $\text{Im}(\epsilon_{yz})$ is the imaginary part of the element. From these results, we ascertained that the diagonal and the off-diagonal elements of the MnAs dielectric tensor were $(2.8 + 4.0i)^2$ and $-1.62 + 0.27i$, respectively, at a wavelength of 1.55 μm .

Using the obtained tensor data of MnAs, we calculated the forward and the backward propagation losses and the nonreciprocity (or isolation ratio) in our isolator as a function of MnAs layer thickness for the 1.55 μm TM mode, where the SOA was not operated (i.e., driving current was 0). In solving eq. (2), we assumed that H_x and E_z showed exponential attenuation in the Au layer and the InP substrate. Figure 4 shows the results. The device shows a large propagation loss and a small isolation ratio for small values of MnAs thickness, because light traveling in the isolator leaks out of the MnAs layer and is absorbed strongly by the

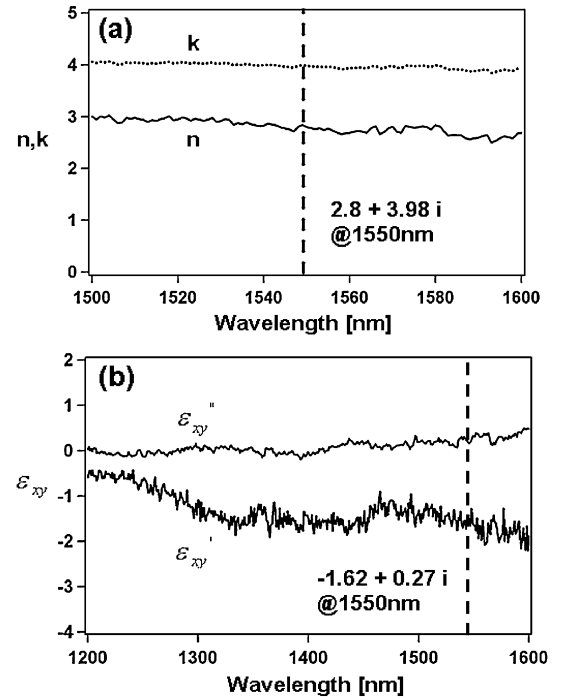


Fig. 3. Optical properties of an MBE-grown, epitaxial MnAs layer: (a) complex refractive index $n + ik$ and (b) off-diagonal element $\epsilon_{yz} = \epsilon_{yz}' + i\epsilon_{yz}''$, plotted as a function of wavelength.

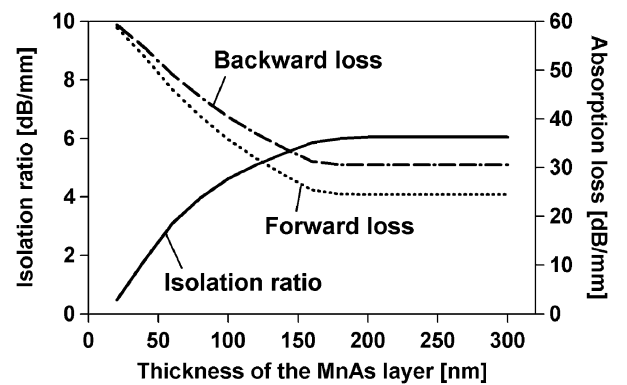


Fig. 4. Forward and backward propagation losses and isolation ratio (nonreciprocity) in the device as a function of MnAs layer thickness, calculated for 1.55 μm TM mode. The isolation ratio saturates at a MnAs layer thickness of 150–200 nm.

Au–Ti electrode. The propagation loss decreases as the MnAs thickness increases and approaches to a certain value determined by absorption in the MnAs layer; the propagation loss is almost constant if the MnAs thickness is larger than 200 nm. This shows that the penetration depth of light in the MnAs layer is about 200 nm. The isolation ratio

increases with an increase in the MnAs thickness and saturates at 6 dB/mm at a thickness of 150–200 nm. From these results, we decided that the necessary and sufficient thickness of the MnAs layer is 200 nm. This thickness is achievable; we can grow a 200-nm-thick MnAs layer on InGaAsP contact layers by MBE.

4. Fabricating the Device

On the basis of the results obtained in the previous sections, we fabricated an actual device as follows. The substrate was a highly doped, [100]-oriented n-type wafer of InP. The SOA was formed on the substrate by metalorganic vapor phase epitaxy (MOVPE). The MQW (see the end of §2 for the structure) showed a photoluminescence peak at 1.54 μm. After the formation of the SOA, a 200 nm MnAs layer was grown on the surface of the InGaAsP contact layer by MBE. To examine the dependence of the nonreciprocity on MnAs thickness, four other devices with MnAs layers of 20, 50, 100, and 150 nm thickness were also prepared. The wafer was first heat treated at about 500–600 °C under As flux in the MBE chamber to remove a native oxide layer on the cladding layer. The wafer temperature was then lowered to 200 °C, and the MnAs layer was grown directly without a buffer layer. Elemental Mn and As solid sources were used to provide Mn and As₄ fluxes, respectively. The growth rate was 80 nm/h. We observed the surface of the wafer by refraction high energy electron diffraction (RHEED) during the growth process and confirmed that the MnAs layer grown was single crystalline.

After the growth of MnAs, a 200-nm-thick SiO₂ layer was deposited on the MnAs layer by magnetron sputtering, and then a stripe window was opened by optical lithography to fabricate a gain-guiding waveguide structure. The width of the window was set to 5.5 μm. A 100 nm Ti layer and a 200 nm Au layer were then deposited on the surface to make a top electrode, by electron-beam (EB) evaporation. In this way, we fabricated the structure given in Fig. 1. Finally, both ends of the device were cleaved to set the device length to 0.65 mm; the cleaved surfaces were left uncoated. Figure 5 shows a cross section of the device observed using a scanning electron microscope (SEM).

The MnAs layer on the device shows strong magnetic anisotropy, and this must be taken into consideration when designing the device. Figure 6 shows a plot of the magnetization curve of the MnAs layer on the device, measured by alternating gradient force magnetometry (AGFM). Using a

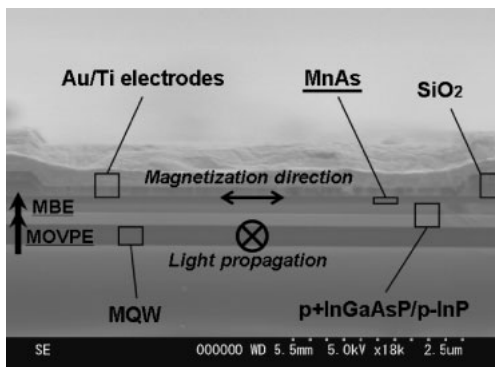


Fig. 5. Cross section of the device observed using a SEM.

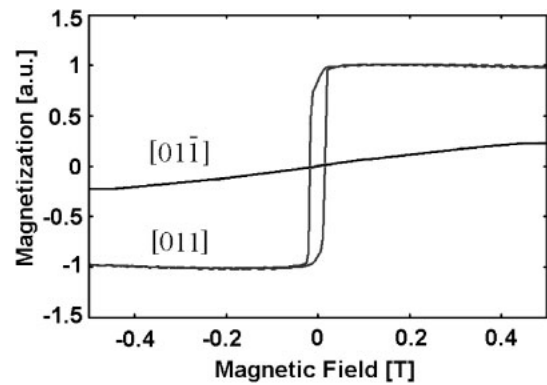


Fig. 6. Magnetization curve for the MnAs layer on the device: the results for a 100-nm-thick MnAs layer, measured by AGFM. The MnAs layer can be easily magnetized using a magnetic field along the [011] direction of the InP substrate. In contrast, magnetization is difficult along the [01 $\bar{1}$] direction of the InP substrate.

magnetic field applied along the [011] direction of the InP substrate, the MnAs layer was easily magnetized by a small coercive field of 0.017 T. In contrast, it was not easy to magnetize the MnAs layer along the [01 $\bar{1}$] direction and even a coercive field of 0.5 T was insufficient. This anisotropy is due to the crystalline anisotropy of the MnAs layer on the InGaAsP. Therefore, to operate the device with a small external magnetic field, we formed the waveguide stripe parallel to the [01 $\bar{1}$] direction of the InP substrate, and magnetized the MnAs layer in the [011] direction (*x* direction in Fig. 1).

5. Device Operation

We confirmed that the device functioned successfully as an optical isolator with nonreciprocal loss for TM-polarized, 1.5 μm light. Our experimental setup for the measurement consisted of a wavelength-tunable laser with a polarization controller, optical circulators and switches, a magnet, an optical power meter, and an optical spectrum analyzer. A tunable laser generated light and sent it to the device through a polarization controller and a circulator. The light was transferred into and out of the device through lensed fibers. A magnetic field was applied using a permanent magnet along the [011] direction of the device, i.e., parallel to the device surface and perpendicular to the direction of light propagation (see Fig. 1). Light propagation in the device was switched between the forward and the backward directions by controlling two optical switches. The intensity of the transmitted light from the device was measured using an optical spectrum analyzer and a power meter. The output of the tunable laser was set to 5 dBm, and the magnetic field for the device was set to 0.1 T.

During measurement, the device was placed in a fixed-temperature box set at 15 °C and operated with a driving current of 100 mA (current density = 2.5 kA/cm²). The voltage drop across the device was 1.7 V. Since our previous device with a Fe/Ni contact electrode had shown a higher voltage drop of 3.0 V,¹⁹⁾ the MnAs layer provided a low-resistance contact, as compared with ordinary ferromagnetic metals.

Figure 7 shows the forward transmission (dashed line) and backward transmission (solid line) in the device,

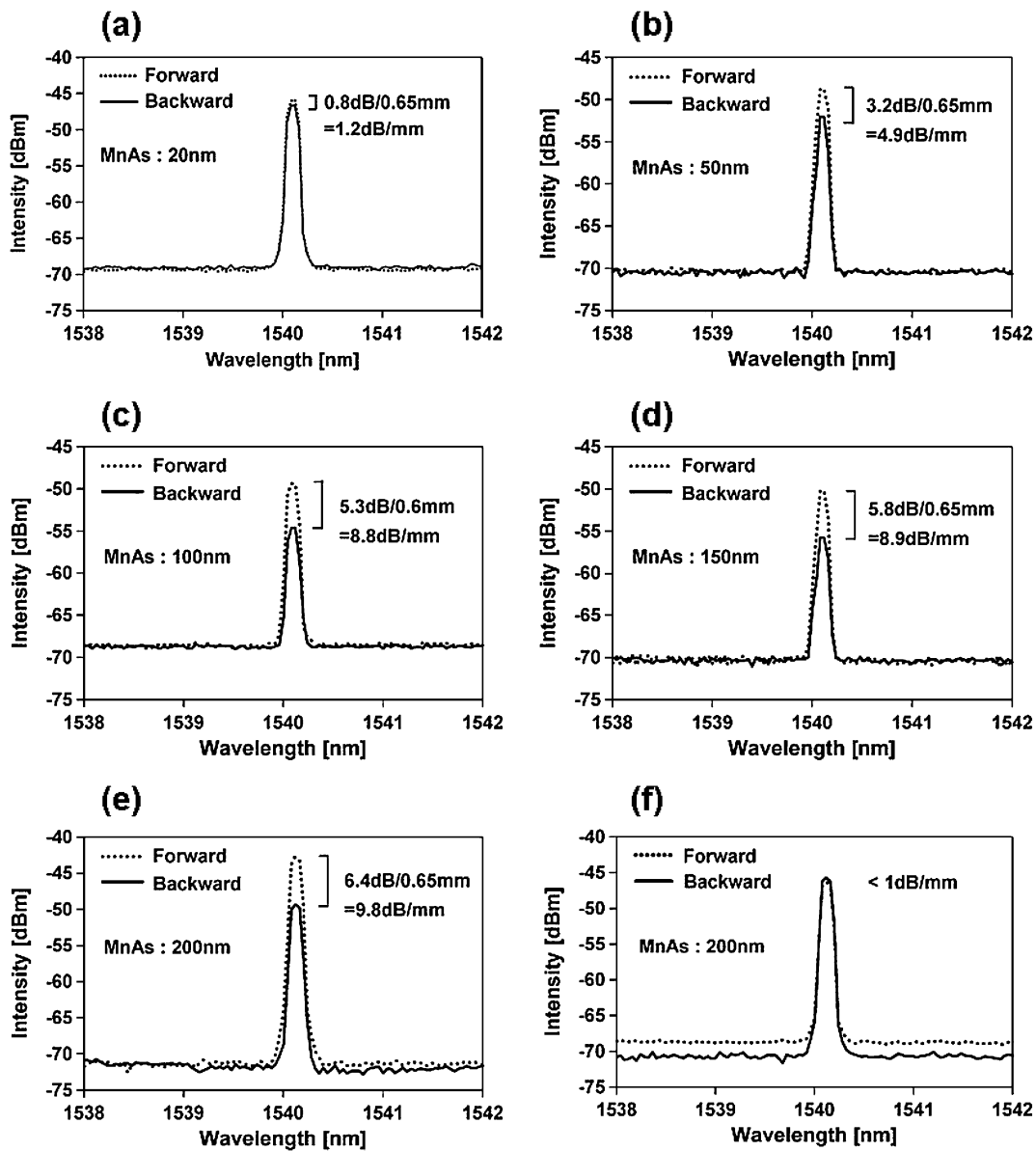


Fig. 7. Forward transmission (dashed line) and backward transmission (solid line) in the device, measured for 1.54 μm TM mode, under a 100 mA driving current and a 0.1 T magnetic field. The thickness of the MnAs layer is (a) 20, (b) 50, (c) 100, (d) 150, and (e) 200 nm. Figure (f) shows a result measured for TE mode, with a 200 nm MnAs layer.

measured for [Figs. 7(a)–7(e)] TM-polarized and [Fig. 7(f)] TE-polarized light. The intensity of light at the output end of the device is plotted as a function of the wavelength for forward and backward propagation. The wavelength of light was fixed at 1.54 μm . In the device with a 200 nm MnAs layer, the output intensity for the TM mode changed by 6.4 dB by switching the direction of light propagation. The device efficiently operated as a TM-mode isolator with an isolation ratio of 9.8 dB/mm (= 6.4 dB/0.6 mm). In contrast, the output intensity for the TE mode had little dependence on the direction of propagation, as expected.

Figure 8 shows a plot of the intensity of transmitted light (for forward and backward propagation) and the isolation ratio as a function of MnAs layer thickness. The incident light was 1.54 μm . The isolation ratio increased monotonically with an increase in MnAs thickness and saturated at a thickness of 150–200 nm—the penetration depth of light in the MnAs layer. This is consistent with the prediction in §3.

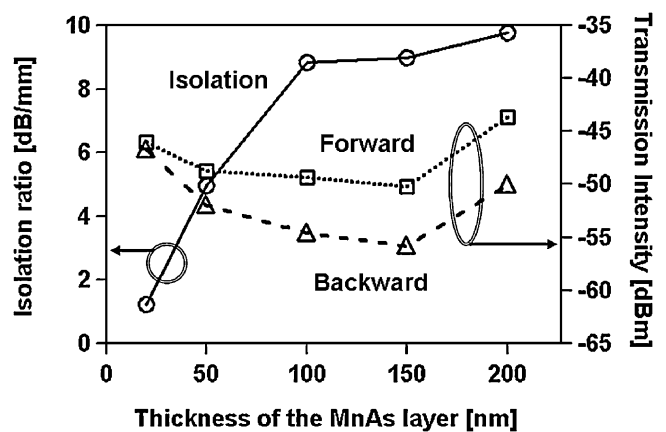


Fig. 8. Forward and backward transmission and isolation ratio as a function of MnAs layer thickness, under a 100 mA driving current and a 0.1 T magnetic field.

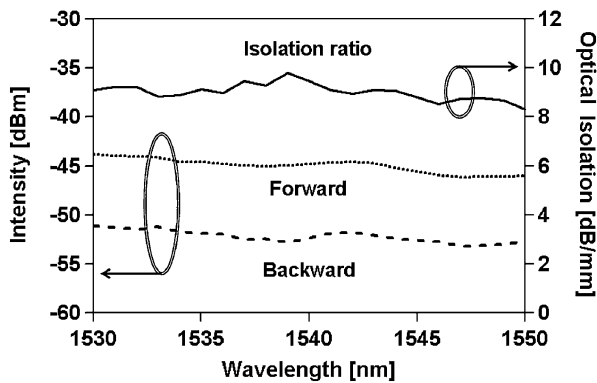


Fig. 9. Forward and backward transmission and isolation ratio as a function of wavelength, measured for the device with a 200 nm MnAs layer.

According to the prediction, the transmission intensity of light should increase monotonically with an increase in the MnAs thickness. Actually, this did not occur as shown in Fig. 8. This is due to the nonuniformity of the coupling loss for the device samples, because the condition of the cleaved facet was not the same among the device samples. On the other hand, the isolation performance is consistent with the simulation results regardless of the coupling loss, because the nonreciprocal loss phenomenon is generated only in the device.

Figure 9 shows a plot of the output intensity for forward and backward propagation and isolation ratio as a function of wavelength from 1.53 to 1.55 μm , measured for the device with a 200 nm MnAs layer. In this range of wavelengths, the isolation ratio was almost constant.

The forward propagation loss observed in this sample device was large, as can be seen in Figs. 8 and 9. This was caused by the fact that the intrinsic propagation loss in the device was about 35 dB, larger than expected. The gain in the SOA was insufficient to compensate for the sum of the intrinsic propagation loss and the measurement system loss (total loss in lensed-fiber couplers, circulators, and switches: about 25 dB in total). To reduce the intrinsic loss of the device, the following two approaches are most promising. The first is to improve the gain in the SOA by increasing the number of well layers in the MQW region. The second approach is to reduce the propagation loss of the device using a ridge waveguide structure with a large confinement factor. We are now developing improved devices with a smaller intrinsic absorption loss.

6. Conclusions

We developed a 1.5- μm -band, TM-mode waveguide isolator. The device consists of a semiconductor active waveguide with a ferromagnetic MnAs layer, making use of the nonreciprocal loss caused by the magneto-optic trans-

verse Kerr effect. The MnAs layer serves a dual function of producing the nonreciprocal effect due to its ferromagnetism and of acting as a low-resistance contact on the semiconductor waveguide. MnAs is more suitable for this purpose than ordinary ferromagnetic metals. The thickness of the MnAs layer affects the optical nonreciprocity and propagation loss in the device. We determined by theory and experiments that the optimum MnAs thickness was about 200 nm for a 1.5- μm -band operation. We fabricated a sample device by MOVPE to fabricate the SOA waveguide and by MBE to form the MnAs layer. The device showed a nonreciprocity (isolation ratio) of 9.8 dB/mm in 1.54 μm TM mode, with a 200 nm MnAs layer. These results mean that we can proceed to developing polarization-independent waveguide isolators to construct photonic integrated circuits.

Acknowledgement

This work was supported by a Grant-in-Aid for Scientific Research in Priority Area "Semiconductor Nanospintronics" (No. 16031204) from the Ministry of Education, Culture, Sports, Science and Technology, Japan.

- 1) H. Dammann, E. Pross, G. Rabe, W. Tolksdorf, and M. Zinke: *Appl. Phys. Lett.* **49** (1986) 1755.
- 2) N. Sugimoto, H. Terui, A. Tate, Y. Katoh, Y. Yamada, A. Sugita, A. Shibukawa, and Y. Inoue: *J. Lightwave Technol.* **14** (1996) 2537.
- 3) H. Yokoi, T. Mizumoto, T. Takano, and N. Shinjo: *Appl. Opt.* **38** (1999) 7409.
- 4) H. Yokoi, T. Mizumoto, N. Shinjo, N. Futakuchi, and Y. Nakano: *Appl. Opt.* **39** (2000) 6158.
- 5) H. Yokoi, T. Mizumoto, and Y. Shoji: *Appl. Opt.* **42** (2003) 6605.
- 6) K. Sakurai, H. Yokoi, T. Mizumoto, D. Miyashita, and Y. Nakano: *Jpn. J. Appl. Phys.* **43** (2004) 1388.
- 7) M. Takenaka and Y. Nakano: *Proc. 11th Int. Conf. Indium Phosphide and Related Materials*, 1999, p. 289.
- 8) W. Zaets and K. Ando: *IEEE Photonics Technol. Lett.* **11** (1999) 1012.
- 9) M. Vanwolleghem, W. Van Parys, D. Van Thourhout, R. Baets, F. Lelarge, O. Gauthier-Lafaye, B. Thedrez, R. Wirijs-Speetjens, and L. Lagae: *Appl. Phys. Lett.* **85** (2004) 3980.
- 10) W. Van Parys, B. Moeyersoon, D. Van Thourhout, R. Baets, M. Vanwolleghem, B. Dagens, J. Decobert, O. L. Gouezigou, D. Make, R. Vanheertum, and L. Lagae: *Appl. Phys. Lett.* **88** (2006) 071115.
- 11) H. Shimizu and Y. Nakano: *Jpn. J. Appl. Phys.* **43** (2004) L1561.
- 12) H. Shimizu and Y. Nakano: *J. Lightwave Technol.* **24** (2006) 38.
- 13) T. Amemiya, H. Shimizu, P. N. Hai, M. Yokoyama, M. Tanaka, and Y. Nakano: *Proc. Optical Fiber Communication Conf., 2006, OFA1*.
- 14) T. Amemiya, H. Shimizu, Y. Nakano, P. N. Hai, M. Yokoyama, and M. Tanaka: *Appl. Phys. Lett.* **89** (2006) 021104.
- 15) M. Tanaka, J. P. Harbison, T. Sands, T. L. Cheeks, and G. M. Rothberg: *J. Vac. Sci. Technol. B* **12** (1994) 1091.
- 16) M. Tanaka, J. P. Harbison, and G. M. Rothberg: *Appl. Phys. Lett.* **65** (1994) 1964.
- 17) M. Yokoyama, S. Ohya, and M. Tanaka: *Appl. Phys. Lett.* **88** (2006) 012504.
- 18) K. Sato, H. Ikekame, M. Akita, and Y. Morishita: *J. Magn. Mater.* **177-181** (1998) 1379.
- 19) T. Amemiya, H. Shimizu, and Y. Nakano: *Proc. 17th Int. Conf. Indium Phosphide and Related Materials*, 2005, p. 303.